

Quantitative Study of Near Equilibrium in Dissociative Mechanism of Nickel in Silicon

*Masayuki YOSHIDA,¹ Hajime KITAGAWA,² Masami MOROOKA,²
Shuji TANAKA²*

¹Yoshida Semiconductor Laboratory, Japan

²Fukuoka Institute of Technology, Japan

Corresponding author: Masayuki Yoshida, Yoshida Semiconductor Laboratory,
2-2-37 Kusagae, Chuo-ku, Fukuoka 810-0045, Japan. E-mail: myoshida@ws.ipc.fit.ac.jp

Abstract

The dissociative mechanism of nickel in silicon has been studied experimentally, assuming the near equilibrium represented by $C_i C_V / C_s = C_i^{\text{eq}} C_V^{\text{eq}} / C_s^{\text{eq}}$, where subscripts i, V, and s represent interstitial nickel atoms, vacancies, and substitutional nickel atoms, respectively, superscript eq represents the thermal equilibrium, and C_A is the concentration of component A. However, the assumption of the near equilibrium has not yet been verified experimentally, because it is difficult to measure C_V in silicon. In the present work, the simultaneous diffusion equations of the dissociative mechanism of nickel in silicon are solved numerically by double-precision FORTRAN without assuming the near equilibrium under the condition of in-diffusion of nickel into a silicon specimen, and the establishment of the near equilibrium is verified. It is also clarified that the near equilibrium is a transitional process which continues until the thermal equilibrium is reached. After the near equilibrium is reached, the very small difference of two nearly equal terms is an important factor in solving the diffusion equations. In other words, high accuracy is necessary to solve the diffusion equations. Concerning this, it is verified that the accuracy of double-precision FORTRAN is sufficiently high to solve the diffusion equations in the present work.

Keywords

near equilibrium, thermal equilibrium, dissociative mechanism, nickel in silicon,
accuracy of double-precision FORTRAN

1. Introduction

In 1964, Yoshida and Furusho [1] studied the diffusion of nickel in silicon at 750~1200 °C and concluded that most of the nickel atoms are located at the interstitial sites. In 1967, Yoshida and Saito [2] further studied the nickel diffusion and concluded that about one thousandth of the total number of nickel atoms are electrically active and are located at the substitutional sites, and that nickel diffuses dissociatively. In 1982, Kitagawa *et al.* [3] reaffirmed experimentally the dissociative mechanism of nickel in silicon.

The dissociative mechanism was first proposed by Frank and Turnbull [4] in 1956 for the diffusion of copper in germanium. They also proposed $C_i C_V / C_s = C_i^{eq} C_V^{eq} / C_s^{eq}$, where subscripts i, V, and s represent interstitial impurity atoms, vacancies, and substitutional impurity atoms, respectively, superscript eq represents the thermal equilibrium, and C_A is the concentration of component A. Penning [5] reported that, if this equation is satisfied, the quasi equilibrium is established in the reaction among interstitial copper atoms, vacancies, and substitutional copper atoms.

It is interesting to see that several different terms are adopted by several researchers in place of quasi equilibrium. Goesele *et al.* [6] and Goesele *et al.* [7] proposed the kick-out mechanism for the diffusion of gold in silicon and assumed that the local equilibrium represented by $C_I C_s / C_i = C_I^{eq} C_s^{eq} / C_i^{eq}$ is established, where subscript I represents self-interstitials. In silicon, both vacancies and self-interstitials coexist in the thermally stable state. Concerning this, Goesele *et al.* [8] reported that the model of Sirtl [9] implies the establishment of the local equilibrium in the reaction of the Frenkel defect formation, which is represented by $C_I C_V = C_I^{eq} C_V^{eq}$. The relation, $C_I C_V = C_I^{eq} C_V^{eq}$, was termed the local dynamical equilibrium by Tan *et al.* [10] and the near equilibrium by Dunham. [11] In the present work, the dissociative mechanism of nickel in silicon is studied and the term of near equilibrium is adopted following Dunham, as shown in the title of the present work. The reason for this is described in Section 3.

In ref. 2, implicitly assuming the near equilibrium represented by $C_i C_V / C_s = C_i^{eq} C_V^{eq} / C_s^{eq}$, the diffusion of nickel in silicon was studied and it was concluded that nickel diffuses dissociatively. However, the assumption of the near equilibrium was not verified experimentally, because it is difficult to measure the concentration of vacancies in silicon.

In the present work, the simultaneous diffusion equations of the dissociative mechanism of nickel in silicon are solved numerically by double-precision FORTRAN without assuming the near equilibrium under the condition of in-diffusion of nickel into a silicon specimen. The present work has two purposes. Purpose 1 is to obtain the relation between the value of the factor for the dissociative mechanism, α_d of eq. (3), and the time at which the near equilibrium is reached. Note that in the study for Purpose 1, the role of near equilibrium in the process of diffusion is clarified. Purpose 2 is to quantitatively investigate the relation between the near equilibrium and the diffusion equation of substitutional nickel atoms from a viewpoint of accuracy of calculation.

Although Morooka and Yoshida [12] and Kitagawa and Yoshida [13] solved the simultaneous diffusion equations of the dissociative mechanism, the kick-out mechanism, and the Frenkel defect formation without assuming the near equilibrium of these reactions, they did not study the near equilibrium in detail.

2. Diffusion Equations without Assuming Near Equilibrium

The dissociative mechanism of nickel in silicon is expressed by the chemical reaction,



In the present work, only the in-diffusion of nickel into a silicon specimen is studied. Therefore, only the sinks and sources of vacancies are taken into account, and we have



It is assumed that the sinks and sources of vacancies are dislocations.

In reactions (1) and (2), $k_{\text{dis}}^{\text{f}}$, $k_{\text{dis}}^{\text{b}}$, k_{V} , and k_{Vg} are the respective rate constants. We have [14]

$$k_{\text{dis}}^{\text{b}} = 4\pi\alpha_{\text{d}}r_{\text{iV}}(D_{\text{i}} + D_{\text{V}}), \quad (3)$$

$$k_{\text{V}} = \frac{2\pi n_{\text{d}}D_{\text{V}}}{\ln(r_{\text{d}}/r_0)}. \quad (4)$$

In eq. (3), α_{d} is a factor for the dissociative mechanism described in Section 1, r_{iV} is the shortest distance for the recombination of an interstitial nickel atom and a vacancy, and D_{A} is the diffusion coefficient of component A. On the basis of the definitions of α_{d} and r_{iV} , $\alpha_{\text{d}}r_{\text{iV}}$ is defined as the effective distance for the recombination of an interstitial nickel atom and a vacancy. In eq. (4), n_{d} is the dislocation density, r_{d} is half of the mean distance of two adjacent dislocation lines, given by

$$r_{\text{d}} = 1/\sqrt{\pi n_{\text{d}}}, \quad (5)$$

and r_0 is the shortest distance from a dislocation for the capture of a vacancy by a dislocation.

The overall reaction rates of reactions (1) and (2), R_{dis} and R_{V} , are given by

$$R_{\text{dis}} = k_{\text{dis}}^{\text{f}}C_{\text{s}} - k_{\text{dis}}^{\text{b}}C_{\text{i}}C_{\text{V}}, \quad (6)$$

$$R_{\text{V}} = k_{\text{V}}C_{\text{V}} - k_{\text{Vg}}. \quad (7)$$

At the thermal equilibrium, we have

$$R_{\text{dis}} = k_{\text{dis}}^{\text{f}}C_{\text{s}}^{\text{eq}} - k_{\text{dis}}^{\text{b}}C_{\text{i}}^{\text{eq}}C_{\text{V}}^{\text{eq}} = 0, \quad (8)$$

$$R_V = k_V C_V^{\text{eq}} - k_{Vg} = 0, \quad (9)$$

resulting in

$$k_{\text{dis}}^f = k_{\text{dis}}^b \frac{C_i^{\text{eq}} C_V^{\text{eq}}}{C_s^{\text{eq}}}, \quad (10)$$

$$k_{Vg} = k_V C_V^{\text{eq}}. \quad (11)$$

From eqs. (7) and (11), we obtain

$$R_V = k_V (C_V - C_V^{\text{eq}}). \quad (12)$$

On the basis of reactions (1) and (2), or eqs. (6) and (12), the diffusion equations of substitutional nickel atoms, interstitial nickel atoms, and vacancies are given by

$$\frac{\partial C_s}{\partial t} = -k_{\text{dis}}^f C_s + k_{\text{dis}}^b C_i C_V = -R_{\text{dis}}, \quad (13)$$

$$\frac{\partial C_i}{\partial t} = D_i \frac{\partial^2 C_i}{\partial x^2} + k_{\text{dis}}^f C_s - k_{\text{dis}}^b C_i C_V, \quad (14)$$

$$\frac{\partial C_V}{\partial t} = D_V \frac{\partial^2 C_V}{\partial x^2} + k_{\text{dis}}^f C_s - k_{\text{dis}}^b C_i C_V + k_V (C_V^{\text{eq}} - C_V). \quad (15)$$

For the in-diffusion of nickel into a silicon specimen of thickness L , eqs. (13)-(15) are solved under the conditions of

$$C_s = C_i = C_V = 0 \quad \text{at } 0 < x < L \quad \text{and } t = 0, \quad (16)$$

$$C_s = C_s^{\text{eq}}, \quad C_i = C_i^{\text{eq}}, \quad C_V = C_V^{\text{eq}} \quad \text{at } x = 0 \text{ and } L \quad \text{and } t \geq 0. \quad (17)$$

3. Diffusion Equation under Assumption of Near Equilibrium

From eqs. (13) and (15), we obtain

$$\frac{\partial}{\partial t} (C_s + C_V) = D_V \frac{\partial^2 C_V}{\partial x^2} + k_V (C_V^{\text{eq}} - C_V). \quad (18)$$

Equation (18) has two unknowns, C_s and C_V . Therefore, one more equation composed of C_s and C_V is necessary to solve eq. (18). For this purpose, reaction (1) is assumed to be in the near equilibrium, and we have from eq. (6)

$$R_{\text{dis}} = k_{\text{dis}}^f C_s - k_{\text{dis}}^b C_i C_V \approx 0. \quad (19)$$

Because $R_{\text{dis}} \approx 0$ is not suitable for mathematical treatment, R_{dis} of eq. (6) is assumed to be $R_{\text{dis}} = 0$, and we have from eqs. (6) and (10)

$$\frac{C_i C_V}{C_s} = \frac{C_i^{\text{eq}} C_V^{\text{eq}}}{C_s^{\text{eq}}}. \quad (20)$$

$R_{\text{dis}} \approx 0$ of eq. (19) is the reason why the term of near equilibrium is adopted in the present work. Exactly speaking, $R_{\text{dis}} = 0$ is satisfied only in the case of eq. (8). It is also assumed that interstitial nickel is in the thermal equilibrium, or

$$C_i = C_i^{\text{eq}}. \quad (21)$$

From eqs. (20) and (21), we obtain

$$C_V = C_s \frac{C_V^{\text{eq}}}{C_s^{\text{eq}}}. \quad (22)$$

Substitution of eq. (22) into eq. (18) yields

$$\frac{\partial C_s}{\partial t} = D_{\text{Vdis}} \frac{\partial^2 C_s}{\partial x^2} + k_{\text{Vdis}} (C_s^{\text{eq}} - C_s), \quad (23)$$

$$D_{\text{Vdis}} = D_V \frac{C_V^{\text{eq}}}{C_V^{\text{eq}} + C_s^{\text{eq}}}, \quad (24)$$

$$k_{\text{Vdis}} = k_V \frac{C_V^{\text{eq}}}{C_V^{\text{eq}} + C_s^{\text{eq}}}. \quad (25)$$

Equation (23) is solved under the conditions of

$$C_s = 0 \quad \text{at } 0 < x < L \quad \text{and } t = 0, \quad (26)$$

$$C_s = C_s^{\text{eq}} \quad \text{at } x = 0 \quad \text{and } L \quad \text{and } t \geq 0. \quad (27)$$

4. Solution of Diffusion Equation under Assumption of Near Equilibrium

Defining ζ_m and ξ_m by

$$\zeta_m = \frac{mL + x}{2\sqrt{D_{\text{Vdis}} t}}, \quad (28)$$

$$\xi_m = \frac{(m+1)L-x}{2\sqrt{D_{\text{vdis}}t}}, \quad (29)$$

the solution of eq. (23) under the conditions of eqs. (26) and (27) is given by

$$\frac{C_s}{C_s^{\text{eq}}} = 1 - \exp(-k_{\text{vdis}}t) \left(1 - \sum_{m=0}^{\infty} (-1)^m [\text{erfc}(\zeta_m) + \text{erfc}(\xi_m)] \right). \quad (30)$$

From eq. (30),

$$\begin{aligned} \frac{1}{C_s^{\text{eq}}} \frac{\partial C_s}{\partial t} &= k_{\text{vdis}} \exp(-k_{\text{vdis}}t) \left(1 - \sum_{m=0}^{\infty} (-1)^m [\text{erfc}(\zeta_m) + \text{erfc}(\xi_m)] \right) \\ &+ \frac{\exp(-k_{\text{vdis}}t)}{2\sqrt{\pi D_{\text{vdis}}t^3}} \sum_{m=0}^{\infty} (-1)^m \{ [mL+x] \exp(-\zeta_m^2) + [(m+1)L-x] \exp(-\xi_m^2) \}. \end{aligned} \quad (31)$$

Equation (31) is used for Purpose 2.

Tanaka and Kitagawa [15] obtained the diffusion profiles of substitutional nickel in silicon, using phosphorus-doped, n-type, dislocation-free FZ silicon. In their experiment, the thickness of specimen is $L = 0.15$ cm, and the diffusion temperature is 980 °C. The diffusion profiles of substitutional nickel at diffusion times of $t = 6.0 \times 10^2$ s, 1.8×10^3 s, and 7.2×10^3 s are shown in Fig. 1.

These experimental profiles are used for simulation by eq. (30) to determine the values of the constants in Section 2. Although dislocation-free silicon was used in the experiment, it was found that the sinks and sources of vacancies in the bulk are necessary for the simulation. Therefore, they are assumed to be dislocations with a dislocation density of n_d .

From eq. (5) of ref. 2, $C_s^{\text{eq}} = 3.39 \times 10^{13}$ cm⁻³ is obtained. From eq. (22) of Yoshida[16] in the study of phosphorus diffusion in silicon, $D_{\text{V}^-} = 1.70 \times 10^{-5}$ cm² s⁻¹ is obtained. For the simulation, $C_s^{\text{eq}} = 3.40 \times 10^{13}$ cm⁻³, $D_{\text{V}} = 1.70 \times 10^{-5}$ cm² s⁻¹, $C_{\text{V}}^{\text{eq}} = 7.00 \times 10^{10}$ cm⁻³, and $n_d = 3.00 \times 10^3$ cm⁻² are adopted. Note that $D_{\text{V}} C_{\text{V}}^{\text{eq}} = 1.19 \times 10^6$ cm⁻¹ s⁻¹ is obtained from the values described above and also from eq. (11) of ref. 2. $r_{\text{iv}} = r_0 = 2.35 \times 10^{-8}$ cm are determined from the distance between nearest-neighbor atoms in the silicon lattice. Using these values, C_s of eq. (30) at $t = 6.0 \times 10^2$ s, 1.8×10^3 s, and 7.2×10^3 s are shown in Fig. 1 for the simulation. It is seen in Fig. 1 that the simulation is good. The three different lines for $\alpha = 10^0$, 10^{-6} , and 10^{-7} in Fig. 1 are explained in Section 6.

Although C_i^{eq} and D_i are not included in eq. (30), they are included in Section 2. Therefore, their values are obtained in this section. We have from Fig. 2 of ref. 1

$$C_i^{\text{eq}} = 6.20 \times 10^{26} \exp(-2.33/kT) \text{ cm}^{-3} \quad (T \text{ in K}) \quad \text{at } 922 \geq T \geq 750 \text{ °C}, \quad (32)$$

$$C_i^{\text{eq}} = 1.26 \times 10^{21} \exp(-0.98/kT) \text{ cm}^{-3} \quad (T \text{ in K}) \quad \text{at } 1100 \geq T \geq 922 \text{ }^\circ\text{C}, \quad (33)$$

where k is the Boltzmann constant in eV/K and T is the temperature. At $T > 1100 \text{ }^\circ\text{C}$, it is difficult to express C_i^{eq} by a formula. Therefore, C_i^{eq} at $T > 1100 \text{ }^\circ\text{C}$ is not shown. Although eqs. (32) and (33) were shown in ref. 13, they were misprinted. Therefore, the corrected formulas are shown in eqs. (32) and (33). From eq. (33), $C_i^{\text{eq}} = 1.44 \times 10^{17} \text{ cm}^{-3}$ is obtained. From ref. 1, we have $D_i = 1.00 \times 10^{-4} \text{ cm}^2\text{s}^{-1}$. These values are adopted for the simulation.

The values of the constants determined in this section are listed in Table I, together with L . The value of $C_i^{\text{eq}} C_V^{\text{eq}} / C_s^{\text{eq}}$, which is used to obtain Normalized $C_i C_V / C_s$ of eq. (41), is also listed in Table I. For the value of α_d of eq. (3), refer to Section 6.

Table I. Values of constants.

C_s^{eq} (cm^{-3})	C_i^{eq} (cm^{-3})	C_V^{eq} (cm^{-3})	$C_i^{\text{eq}} C_V^{\text{eq}} / C_s^{\text{eq}}$ (cm^{-3})	D_i (cm^2s^{-1})	D_V (cm^2s^{-1})
3.40×10^{13}	1.44×10^{17}	7.00×10^{10}	2.96×10^{14}	1.00×10^{-4}	1.70×10^{-5}

n_d (cm^{-2})	r_{iV} (cm)	r_0 (cm)	L (cm)
3.00×10^3	2.35×10^{-8}	2.35×10^{-8}	1.50×10^{-1}

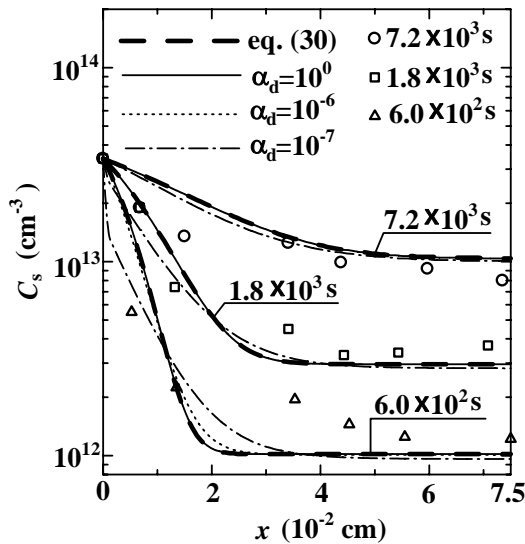


Fig. 1. Experimental profiles of C_s at $980 \text{ }^\circ\text{C}$ and their simulation. The main parameter is the diffusion time, $t = 6.0 \times 10^2 \text{ s}$, $1.8 \times 10^3 \text{ s}$, and $7.2 \times 10^3 \text{ s}$. The specimen thickness is $L = 0.15 \text{ cm}$. For the simulation, C_s of eq. (30) and the general solutions of C_s for $\alpha_d = 10^0$, 10^{-6} , and 10^{-7} are shown.

5. Single Diffusion of Interstitial Nickel Atoms and Vacancies

Diffusion equations for the single diffusion of interstitial nickel atoms and vacancies are given by

$$\frac{\partial C_i}{\partial t} = D_i \frac{\partial^2 C_i}{\partial x^2}, \quad (34)$$

$$\frac{\partial C_v}{\partial t} = D_v \frac{\partial^2 C_v}{\partial x^2} + k_v (C_v^{\text{eq}} - C_v). \quad (35)$$

Equations (34) and (35) are solved under the conditions of

$$C_i = C_v = 0 \quad \text{at } 0 < x < L \quad \text{and } t = 0, \quad (36)$$

$$C_i = C_i^{\text{eq}}, \quad C_v = C_v^{\text{eq}} \quad \text{at } x = 0 \text{ and } L \quad \text{and } t \geq 0. \quad (37)$$

Solutions are

$$\frac{C_i}{C_i^{\text{eq}}} = \sum_{m=0}^{\infty} (-1)^m \left[\operatorname{erfc}\left(\frac{mL+x}{2\sqrt{D_i t}}\right) + \operatorname{erfc}\left(\frac{(m+1)L-x}{2\sqrt{D_i t}}\right) \right]. \quad (38)$$

$$\frac{C_v}{C_v^{\text{eq}}} = 1 - \exp(-k_v t) \left(1 - \sum_{m=0}^{\infty} (-1)^m \left[\operatorname{erfc}\left(\frac{mL+x}{2\sqrt{D_v t}}\right) + \operatorname{erfc}\left(\frac{(m+1)L-x}{2\sqrt{D_v t}}\right) \right] \right). \quad (39)$$

6. Numerical Solutions of Diffusion Equations without Assuming Near Equilibrium

Equations (13)-(15) are solved numerically by double-precision FORTRAN under the conditions of eqs. (16) and (17), applying the Crank-Nicolson implicit method and the Gauss-Seidel iterative method [17] and adopting the values listed in Table I. For α_d of eq. (3), we have

$$\alpha_d = 10^n, \quad (40)$$

where n is an integer from 0 to -12. Hereafter, the solutions of C_s , C_i , and C_v thus obtained are termed the general solutions of C_s , C_i , and C_v , and in this section, for simplicity, they are termed only C_s , C_i , and C_v . Note that C_s obtained from eq. (30), for example, is termed C_s of eq. (30).

It was found that at $t \geq 10^2$ s, C_s for α_d from 10^0 to 10^{-5} are nearly equal to C_s of eq. (30). Therefore, C_s for $\alpha_d = 10^0$ is shown in Fig. 1. It was also found that C_s for $\alpha_d = 10^{-6}$ at $t = 6.0 \times 10^2$ s and C_s for $\alpha_d = 10^{-7}$ at $t = 6.0 \times 10^2$ s, 1.8×10^3 s, and 7.2×10^3 s deviate slightly from C_s of eq. (30). Therefore, they are shown in Fig. 1. Because

C_s for $\alpha_d \leq 10^{-8}$ deviate considerably from C_s of eq. (30), they are not shown in Fig. 1.

To investigate the deviation of C_s from C_s of eq. (30) with the decrease in α_d , the time dependences of C_s of eq. (30) and C_s for $\alpha_d = 10^0$ and $\leq 10^{-6}$ at $x = L/2$ are shown in Fig. 2. It is seen that C_s for $\alpha_d \leq 10^{-8}$ deviate clearly from C_s of eq. (30) and that C_s for $\alpha_d \leq 10^{-9}$ decrease almost proportionally to α_d with the decrease in α_d .

Figure 3 shows the time dependences of C_i of eq. (38) and C_i for $\alpha_d = 10^0$ at $x = L/2$. It is seen that they are nearly equal. Because the time dependences of C_i for α_d from 10^0 to 10^{-12} at $x = L/2$ are nearly equal, only that for $\alpha_d = 10^0$ is shown. These results show that the diffusion of interstitial nickel atoms is not affected by the dissociative mechanism.

Figure 4 shows the time dependences of C_v of eq. (39) and C_v for several values of α_d at $x = L/2$. It is seen that at $t > 2 \times 10^0$ s, C_v for $\alpha_d = 10^0$ deviates considerably from C_v of eq. (39). After this time, the deviation from C_v of eq. (39) gradually decreases with the decrease in α_d , and C_v for $\alpha_d = 10^{-12}$ is nearly equal to C_v of eq. (39). This means that the effect of the dissociative mechanism on the diffusion of vacancies disappears at $\alpha_d = 10^{-12}$.

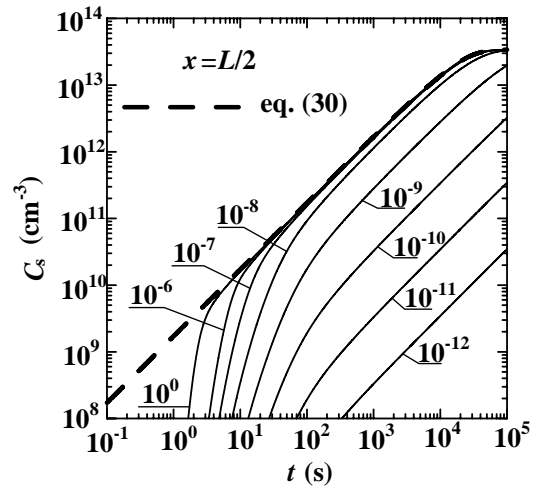


Fig. 2. Time dependences of C_s of eq. (30) and general solution of C_s at $x = L/2$. The parameter is α_d .

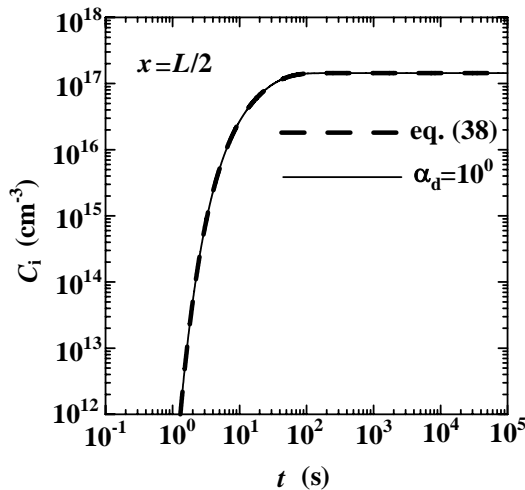


Fig. 3. Time dependences of C_i of eq. (38) and general solution of C_i for $\alpha_d = 10^0$ at $x = L/2$

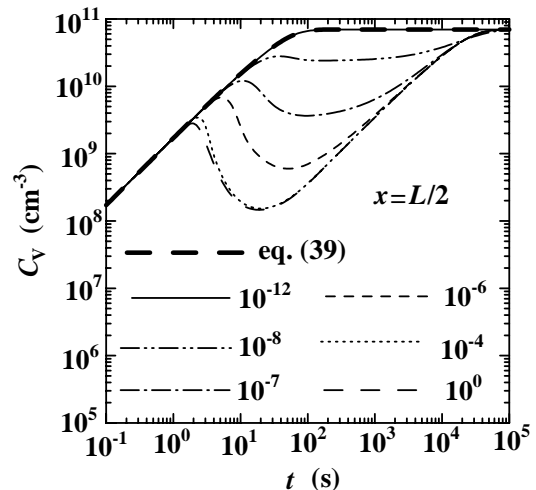


Fig. 4. Time dependences of C_v of eq. (39) and general solution of C_v at $x = L/2$. The parameter is α_d .

Yoshida [18] studied the criteria for the assumptions of the thermal equilibrium of interstitial impurity atoms and vacancies in the dissociative mechanism. He emphasized that the thermal equilibrium concentration, as well as the diffusion coefficient, is an important factor for the criteria. If the diffusion coefficient of interstitial impurity atoms is higher than that of vacancies and other factors are the same, interstitial impurity atoms reach the thermal equilibrium more rapidly than vacancies. [5] In the case of the in-diffusion of impurity atoms, if the thermal equilibrium concentration of interstitial impurity atoms is higher than that of vacancies and other factors are the same, the relative decrease in the concentration of interstitial impurity atoms caused by recombination with vacancies is smaller than that of vacancies, and interstitial impurity atoms reach the thermal equilibrium more rapidly than vacancies. On the basis of these criteria, if $D_i C_i^{\text{eq}} > D_v C_v^{\text{eq}}$ is satisfied, interstitial impurity atoms reach the thermal equilibrium more rapidly than vacancies. From the values listed in Table I, this is satisfied, and C_i for $\alpha_d = 10^0$ reaches the thermal equilibrium value more rapidly than C_v for $\alpha_d = 10^0$, as seen in Figs. 3 and 4.

7. Establishment of Near Equilibrium

On the basis of eqs. (19) and (20), Normalized $C_i C_v / C_s$ is defined as

$$\text{Normalized } C_i C_v / C_s = \frac{k_{\text{dis}}^b C_i C_v}{k_{\text{dis}}^f C_s} = \frac{C_i C_v / C_s}{C_i^{\text{eq}} C_v^{\text{eq}} / C_s^{\text{eq}}}. \quad (41)$$

If Normalized $C_i C_v / C_s \approx 1$ is satisfied, that is, if eq. (19) is satisfied, the near equilibrium is established in the dissociative mechanism.

Purpose 1 of the present work is to obtain the relation between the value of α_d and the time at which the near equilibrium is reached. Substituting the general solutions of C_s , C_i , and C_v into eq. (41), the time dependence of Normalized $C_i C_v / C_s$ at $x = L/2$ is obtained and is shown in Fig. 5, where the parameter is n of $\alpha_d = 10^n$ of eq. (40). When Normalized $C_i C_v / C_s$ changes from 1.01 to 1.00 at $t = t^{\text{ne}}$ with increasing t , t^{ne} is defined as the time at which the near equilibrium is reached. t^{ne} is shown by a circle in Fig. 5 and is also listed in Table II as a function of α_d . In the case of $\alpha_d = 10^0$, the near equilibrium is reached at $t^{\text{ne}} = 5.5 \times 10^{-1}$ s. Note that the effective distance for the recombination of an interstitial nickel atom and a vacancy defined in Section 2 is $\alpha_d r_{iv} = 2.35 \times 10^{-8}$ cm at $\alpha_d = 10^0$. In the case of $\alpha_d \leq 10^{-8}$, the near equilibrium is not yet reached at $t = 10^5$ s. Therefore, t^{ne} for $\alpha_d \leq 10^{-8}$ is not listed in Table II.

To investigate the detail of how the near equilibrium is reached, the time dependences of the general solutions of C_s , C_i , and C_v , and Normalized $C_i C_v / C_s$ at $x = L/2$ and $\alpha_d = 10^0$ are listed in Table III. It is seen that, even if C_s , C_i , and C_v are much smaller than their thermal equilibrium values at $t = 0.55$ s, the near equilibrium is reached. Although not listed in Table III, C_s , C_i , and C_v reach their thermal equilibrium values at $t = 1.1 \times 10^5$ s, 1.4×10^2 s, and 1.2×10^5 s, respectively. The near equilibrium is a transitional process which continues until the thermal equilibrium is reached. This is the role

of near equilibrium in the process of diffusion. Figure 5 and Table III show the transitional process described above.

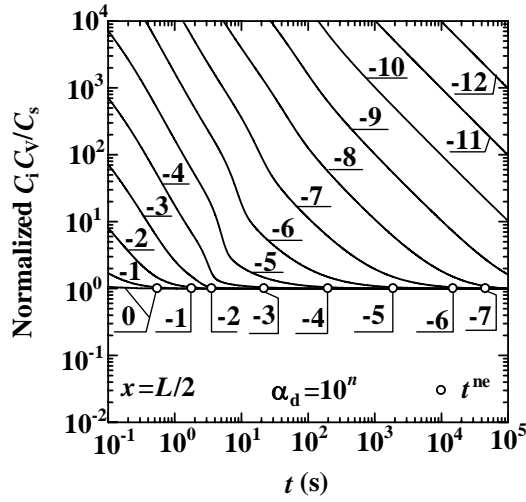


Fig. 5. Time dependence of Normalized $C_i C_V / C_s$ at $x=L/2$. The parameter is n of $\alpha_d = 10^n$. t^{ne} is shown by a circle.

Table II. Relation between α_d and t^{ne} at $x=L/2$.

α_d	10^0	10^{-1}	10^{-2}	10^{-3}
t^{ne} (s)	5.5×10^{-1}	1.8×10^0	3.6×10^0	2.2×10^1
α_d	10^{-4}	10^{-5}	10^{-6}	10^{-7}
t^{ne} (s)	2.0×10^2	1.9×10^3	1.5×10^4	4.6×10^4

Table III. Time dependences of general solutions of C_s , C_i , and C_V , and Normalized $C_i C_V / C_s$ at $x=L/2$ and $\alpha_d = 10^0$.

t (s)	C_s (cm^{-3})	C_i (cm^{-3})	C_V (cm^{-3})	Normalized $C_i C_V / C_s$
0.10	2.03×10^{-36}	3.74×10^{-30}	1.72×10^8	1.07
0.50	1.05×10^{-1}	3.63×10^4	8.58×10^8	1.01
0.55	1.32×10^0	4.17×10^5	9.43×10^8	1.00
10^0	2.06×10^5	3.59×10^{10}	1.71×10^9	1.00
10^1	1.62×10^{10}	2.69×10^{16}	1.79×10^8	1.00
10^2	1.71×10^{11}	1.42×10^{17}	3.58×10^8	1.00
10^3	1.68×10^{12}	1.44×10^{17}	3.46×10^9	1.00
10^4	1.37×10^{13}	1.44×10^{17}	2.82×10^{10}	1.00
10^5	3.39×10^{13}	1.44×10^{17}	6.99×10^{10}	1.00

It is seen in Fig. 1 that the general solutions of C_s for $\alpha_d = 10^{-6}$ and 10^{-7} at $t = 6.0 \times 10^2$ s deviate from C_s of eq. (30). It is also seen in Fig. 5 that at $x = L/2$ and $t = 6.0 \times 10^2$ s, the near equilibrium is not yet established in the case of $\alpha_d \leq 10^{-5}$. Therefore, it is expected that the deviation of the general solutions of C_s described above is caused by the nonestablishment of the near equilibrium.

To verify this, Normalized $C_i C_V / C_s$ for $\alpha_d = 10^0, 10^{-6}, 10^{-7},$ and 10^{-8} at $0 \leq x \leq 7.5 \times 10^{-2}$ cm and $t = 6.0 \times 10^2$ s are shown in Fig. 6. In these ranges of x and t , we have Normalized $C_i C_V / C_s \approx 1.00$ at α_d from 10^0 to 10^{-4} and ≈ 1.02 at $\alpha_d = 10^{-5}$. Therefore, Normalized $C_i C_V / C_s$ for α_d from 10^{-1} to 10^{-5} are not shown in Fig. 6. Comparing Fig. 1 with Fig. 6, it is verified that the deviation of the general solutions of C_s from C_s of eq. (30) is caused by the nonestablishment of the near equilibrium.

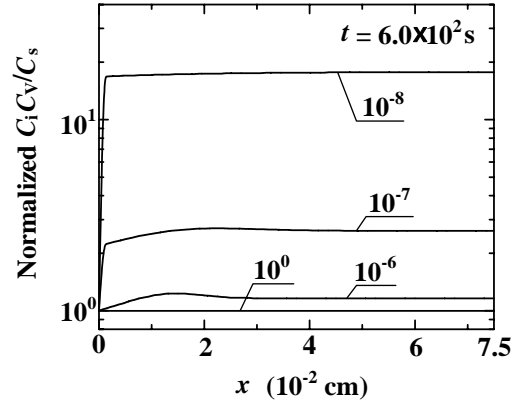


Fig. 6. Dependence of Normalized $C_i C_V / C_s$ on x at $t = 6.0 \times 10^2$ s. The parameter is α_d .

Next, we investigate the relation between eqs. (13) and (31) from the viewpoint of accuracy of calculation. This is Purpose 2. As described in Section 6, the simultaneous diffusion equations of eqs. (13)-(15) are solved numerically by double-precision FORTRAN. When the near equilibrium is established, we have $k_{\text{dis}}^f C_s \approx k_{\text{dis}}^b C_i C_V$ from eq. (19), and the very small difference, $-k_{\text{dis}}^f C_s + k_{\text{dis}}^b C_i C_V$, gives $-R_{\text{dis}}$ and $\partial C_s / \partial t$ of eq. (13). In Purpose 2, it is investigated whether or not the accuracy of $-R_{\text{dis}}$ of eq. (13) is sufficiently high for solving eqs. (13)-(15). Note that under the assumption of near equilibrium, $\partial C_s / \partial t$ is also given by eq. (31).

For Purpose 2, $k_{\text{dis}}^f C_s$, $k_{\text{dis}}^b C_i C_V$, $-R_{\text{dis}}$, and Normalized $C_i C_V / C_s$ at $x = L/2$ and $t = 10^5$ s are listed in Table IV, where the parameter is α_d . Because the numerical values of $k_{\text{dis}}^f C_s$ and $k_{\text{dis}}^b C_i C_V$ for the same value of α_d are nearly equal, their numerical values have a space to obtain their difference, $-R_{\text{dis}}$, easily. At $\alpha_d = 10^0$, $k_{\text{dis}}^f C_s$ and $k_{\text{dis}}^b C_i C_V$ are on the order of 10^{17} and their difference, $-R_{\text{dis}}$, is on the order of 10^6 . Therefore the numerical values of $k_{\text{dis}}^f C_s$ and $k_{\text{dis}}^b C_i C_V$ have the space after the first 11 digits.

In Table IV, with the increase in α_d , $k_{\text{dis}}^f C_s$ and $k_{\text{dis}}^b C_i C_V$ increase almost proportionally to α_d , but their difference, $-R_{\text{dis}}$, converges to a constant value of $3.89 \times 10^6 \text{ cm}^{-3} \text{ s}^{-1}$. Therefore, the highest accuracy is necessary at the largest value of α_d , or at $\alpha_d = 10^0$, to obtain a correct value of $-R_{\text{dis}}$. The increase in $k_{\text{dis}}^f C_s$ and $k_{\text{dis}}^b C_i C_V$ described above will be discussed in the final part of this section. At $\alpha_d = 10^0$, because Normalized $C_i C_V / C_s$ is 1.00 and the near equilibrium is established, values of $-R_{\text{dis}}$ and

$\partial C_s / \partial t$ of eq. (13) and $\partial C_s / \partial t$ of eq. (31) should be equal to each other. Although not listed in Table IV, we have $\partial C_s / \partial t = 3.89 \times 10^6 \text{ cm}^{-3} \text{ s}^{-1}$ of eq. (31), which is equal to $-R_{\text{dis}}$ and $\partial C_s / \partial t$ of eq. (13) for $\alpha_d = 10^0$. Therefore, the accuracy of calculation by double-precision FORTRAN is sufficiently high for the present work. This accuracy is verified in the appendix, too, in which the accuracy of a very small difference of two nearly equal terms is investigated directly.

Table IV. Dependences of $k_{\text{dis}}^f C_s$, $k_{\text{dis}}^b C_i C_V$, $-R_{\text{dis}}$, and Normalized $C_i C_V / C_s$ on α_d at $x = L/2$ and $t = 10^5 \text{ s}$. Numerical values of $k_{\text{dis}}^f C_s$ and $k_{\text{dis}}^b C_i C_V$ have a space to obtain their difference, $-R_{\text{dis}}$, easily.

α_d	$k_{\text{dis}}^f C_s$ ($\text{cm}^{-3} \text{ s}^{-1}$) $k_{\text{dis}}^b C_i C_V$ ($\text{cm}^{-3} \text{ s}^{-1}$)	$-R_{\text{dis}}$ ($\text{cm}^{-3} \text{ s}^{-1}$)	Normalized $C_i C_V / C_s$
10^0	3.4767332005 4063 $\times 10^{17}$ 3.4767332005 7950 $\times 10^{17}$	3.89×10^6	1.00
10^{-1}	3.476733220 43444 $\times 10^{16}$ 3.476733220 82306 $\times 10^{16}$	3.89×10^6	1.00
10^{-2}	3.47673318 079489 $\times 10^{15}$ 3.47673318 468110 $\times 10^{15}$	3.89×10^6	1.00
10^{-3}	3.4767329 9456175 $\times 10^{14}$ 3.4767330 3342484 $\times 10^{14}$	3.89×10^6	1.00
10^{-4}	3.476730 66849826 $\times 10^{13}$ 3.476731 05725640 $\times 10^{13}$	3.89×10^6	1.00
10^{-5}	3.47670 753623606 $\times 10^{12}$ 3.47671 143646226 $\times 10^{12}$	3.90×10^6	1.00
10^{-6}	3.4764 7322707852 $\times 10^{11}$ 3.4765 1350514929 $\times 10^{11}$	4.03×10^6	1.00
10^{-7}	3.473 77561009421 $\times 10^{10}$ 3.474 31978460946 $\times 10^{10}$	5.44×10^6	1.00
10^{-8}	3.4 0452304940905 $\times 10^9$ 3.4 3477157514792 $\times 10^9$	3.02×10^7	1.01
10^{-9}	2.02044231924644 $\times 10^8$ 3.26092120645935 $\times 10^8$	1.24×10^8	1.61

To see the overall relation between $-R_{\text{dis}}$ of eq. (13) and $\partial C_s / \partial t$ of eq. (31), their time dependences at $x=L/2$ are shown in Fig. 7, where the parameter is α_d . At $t > 10^2$ s, $-R_{\text{dis}}$ for $\alpha_d = 10^0$ agrees well with $\partial C_s / \partial t$ of eq. (31). Because $-R_{\text{dis}}$ for α_d from 10^{-1} to 10^{-5} agree well with that for $\alpha_d = 10^0$ at $t > 10^2$ s, they are not shown. At $10^2 \leq t \leq 10^4$ s, $-R_{\text{dis}}$ for $\alpha_d \leq 10^{-9}$ decrease almost proportionally to α_d . At $t = 10^5$ s, $-R_{\text{dis}}$ increases with the decrease in α_d from 10^0 to 10^{-9} then it decreases with the decrease in α_d from 10^{-9} to 10^{-12} . The increase in $-R_{\text{dis}}$ described above is also seen in Table IV.

As described before, $k_{\text{dis}}^f C_s$ and $k_{\text{dis}}^b C_i C_V$ listed in Table IV increase almost proportionally to α_d with the increase in α_d . Because the near equilibrium is established with the increase in α_d , the values of C_s of $k_{\text{dis}}^f C_s$ in Table IV converge to a constant value given by eq. (30), resulting in a nearly constant value of $C_i C_V$ of eq. (20). As seen in eqs. (3) and (10), k_{dis}^b and k_{dis}^f are proportional to α_d . Therefore, $k_{\text{dis}}^f C_s$ and $k_{\text{dis}}^b C_i C_V$ are almost proportional to α_d .

8. Conclusions

In the experimental study of the dissociative mechanism of nickel in silicon, the near equilibrium is assumed. However, it is difficult to verify the near equilibrium experimentally.

In the present work, the simultaneous diffusion equations of the dissociative mechanism of nickel in silicon are solved numerically by double-precision FORTRAN without assuming the near equilibrium, and the establishment of the near equilibrium is verified. In the case of $C_s^{\text{eq}} = 3.40 \times 10^{13} \text{ cm}^{-3}$, $C_i^{\text{eq}} = 1.44 \times 10^{17} \text{ cm}^{-3}$, $C_V^{\text{eq}} = 7.00 \times 10^{10} \text{ cm}^{-3}$, $D_i = 1.00 \times 10^{-4} \text{ cm}^2 \text{ s}^{-1}$, $D_V = 1.70 \times 10^{-5} \text{ cm}^2 \text{ s}^{-1}$, and $\alpha_d r_{iV} = 2.35 \times 10^{-8} \text{ cm}$, the near equilibrium is reached at $t^{\text{ne}} = 5.5 \times 10^{-1} \text{ s}$. It is clarified that the near equilibrium is a transitional process which continues until the thermal equilibrium is reached.

After the near equilibrium is reached, the very small difference of two nearly equal terms is an important factor in solving the diffusion equations. In other words, high accuracy is necessary to solve the diffusion equations. It is verified that the accuracy of double-precision FORTRAN is sufficiently high in the case of the numerical values described above.

Acknowledgement

The authors would like to express their sincere thanks to Professor T. Kato of Fukuoka Institute of Technology for his discussions.

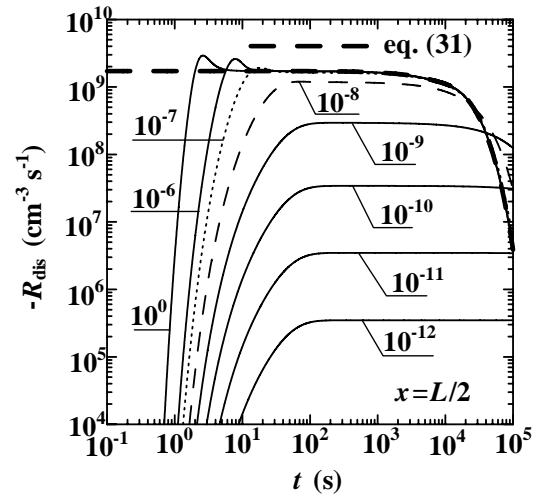


Fig. 7. Time dependences of $\partial C_s / \partial t$ of eq. (31) and $-R_{\text{dis}}$ at $x=L/2$. The parameter is α_d .

Appendix: Accuracy of Calculation

The purpose of the appendix is to directly investigate the accuracy of the very small difference of two nearly equal terms in Table IV, which are obtained by double-precision FORTRAN. For this purpose, the following calculation is done.

Mathematically we have

$$(a + c) - a = c. \quad (\text{A}\cdot 1)$$

The following values are used,

$$\begin{aligned} a &= \sqrt{3} = 1.73205080756888, \\ b &= \sqrt{2} = 1.41421356237310, \\ c &= b \times 10^j, \end{aligned} \quad (\text{A}\cdot 2)$$

where j is an integer. For the purpose of the appendix, f and g are defined as

$$f = a + c, \quad (\text{A}\cdot 3)$$

$$g = f - a. \quad (\text{A}\cdot 4)$$

c of eq. (A.2), f of eq. (A.3), and g of eq. (A.4) are calculated by double-precision FORTRAN. g is then compared with c . Mathematically, g should be equal to c . The difference of g from c is caused by an error in the numerical calculation.

In the case of $\alpha_d = 10^0$ in Table IV, we have $-R_{\text{dis}} / k_{\text{dis}}^f C_s \approx 10^{-11}$. This corresponds to $j = -11$ of eq. (A.2). Therefore, c and g for j from -9 to -13 are listed in Table A.I. Because the numerical values of c and g for the same value of j are nearly equal, their numerical values have a space to see their difference easily.

In Table A.I, the first 5 digits of c and g are equal at $j = -11$, showing that the first 5 digits of g are correct. Therefore, it is verified that the first 3 digits of $-R_{\text{dis}} = 3.89 \times 10^6 \text{ cm}^{-3} \text{ s}^{-1}$ are correct. Note that this value is given also by $\partial C_s / \partial t$ of eq. (31), showing that this value is correct.

Table A.I. Dependences of c and g on j of eq. (A.2). The numerical values of c and g have a space to see their difference easily.

j	c	g
-9	1.414213 56237310 $\times 10^{-9}$	1.414213 63508698 $\times 10^{-9}$
	1.414213 56237310 $\times 10^{-10}$	1.414213 19099777 $\times 10^{-10}$
-11	1.4142 1356237310 $\times 10^{-11}$	1.4142 2429322802 $\times 10^{-11}$
	1.4142 1356237310 $\times 10^{-12}$	1.4142 0208876752 $\times 10^{-12}$
-13	1.414 21356237310 $\times 10^{-13}$	1.414 42413337245 $\times 10^{-13}$
	1.414 21356237310 $\times 10^{-13}$	1.414 42413337245 $\times 10^{-13}$

References

- [1] M. Yoshida and K. Furusho, *Jpn. J. Appl. Phys.* 3 (1964) 521.
- [2] M. Yoshida and K. Saito, *Jpn. J. Appl. Phys.* 6 (1967) 573.
- [3] H. Kitagawa, K. Hashimoto, and M. Yoshida, *Jpn. J. Appl. Phys.* 21 (1982) 276.
- [4] F. C. Frank and D. Turnbull, *Phys. Rev.* 104 (1956) 617.
- [5] P. Penning, *Philips Res. Rep.* 13 (1958) 17.
- [6] U. Goesele, W. Frank, and A. Seeger, *Appl. Phys.* 23 (1980) 361.
- [7] U. Goesele, F. Morehead, W. Frank, and A. Seeger, *Appl. Phys. Lett.* 38 (1981) 157.
- [8] U. Goesele, W. Frank, and A. Seeger, *Solid State Commun.* 45 (1983) 31.
- [9] E. Sirtl, in: H. R. Huff and E. Sirtl (Eds.), *Semiconductor Silicon 1977*, The Electrochemical Society, Princeton, 1977, p. 4.
- [10] T. Y. Tan, F. Morehead, and U. Goesele, in: W. M. Bullis and L. C. Kimerling (Eds.), *Defects in Silicon*, The Electrochemical Society, 1983, p. 325.
- [11] S. T. Dunham, *J. Electrochem. Soc.* 139 (1992) 2628.
- [12] M. Morooka and M. Yoshida, *Jpn. J. Appl. Phys.* 28 (1989) 457.
- [13] H. Kitagawa and M. Yoshida, *Jpn. J. Appl. Phys.* 31 (1992) 2859.
- [14] A. C. Damask and G. J. Dienes, *Point Defects in Metals*, Gordon and Breach, New York, 1963, p. 81.
- [15] S. Tanaka and H. Kitagawa, *Res. Bull. Fukuoka Inst. Tech.* 39 (2006) 13.
- [16] M. Yoshida, *Jpn. J. Appl. Phys.* 18 (1979) 479.
- [17] G. D. Smith, *Numerical Solution of Partial Differential Equations*, Oxford University Press, London, 1974, p. 17 and p. 24.
- [18] M. Yoshida, *Jpn. J. Appl. Phys.* 8 (1969) 1211.